

MICROMECHANICS AS A VIRTUAL TESTING TOOL TO UNDERSTAND DAMAGE BEHAVIOURS OF CONTINUOUS FIBRE-REINFORCED THERMOPLASTIC COMPOSITES

Ditho A. Pulungan¹, Gilles Lubineau¹, Arief Yudhanto¹, Recep Yaldiz², and Warden Schijve²

¹King Abdullah University of Science and Technology (KAUST), Physical Science and Engineering Division, COHMAS Laboratory, Thuwal 23955-6900, Saudi Arabia

Email: gilles.lubineau@kaust.edu.sa, Web Page: <http://cohmas.kaust.edu.sa>

²Sabic T&I Corporate Research & Development, Composites,
P.O Box 319, 6160 AH Geleen, The Netherlands

Keywords: Micromechanics, Damage, RVE development, thermoplastic composites, virtual testing

Abstract

A micromechanical approach was utilized to predict damage mechanisms in glass fibre/polypropylene (GF/PP) thermoplastic composites. First, we systematically determine a representative volume element (RVE) of such materials using a two-point probability function and the eigenvalue stabilization of homogenized elastic tensor. Next, the 3D finite element models of the RVE were developed accordingly. We implemented a set of constitutive models capable of describing the behaviour of GF/PP under various loading conditions with the focus on pressure- and rate-dependent behaviours of polypropylene. The RVE was then imposed with periodical boundary conditions and subjected to transverse tensile loading accordance with experimental tensile tests on $[90]_8$ laminates. The simulation results were in excellent agreement with experiments including the nonlinearity and the failure point, making it a useful virtual testing tool for composite material design. The effects of the main parameters that can be tailored in such materials were then investigated to provide guidelines for future improvements of the materials. It was found that increasing matrix ductility is not an effective strategy to improve the strength and ductility of the composite while increasing the inter-fibre distance could significantly delay the initiation of a transverse crack.

1. Introduction

Recently, thermoplastic composite gains significant interest in the automotive industry due to their lightweight, fast processing time, and excellent impact resistance [1]. The impact performance of the thermoplastic composites is primarily driven by both the behaviour of their constituents (ductility and time-dependent behaviour of the thermoplastic matrix) and the microstructures of the tape. To design thermoplastic composites with superior impact performance, manufacturing industries need to have a robust numerical tool to very quickly virtually test the influence of microstructural design parameters on the damage behaviour of composites. Such a tool will give insight on how to improve material performance that would be difficult to obtain from experiments which are very costly and time-consuming.

In laminated composites, damage evolves through various length scales (*i.e.* from the scale of fibre to that of structures). A pyramidal approach is usually employed to thoroughly understand how damage may initiate at a lower scale and then propagate toward a higher scale [2]. Here we focus on the first stage of the pyramidal approach: micromechanics. Many researchers have successfully developed micromechanical models for fibre-reinforced composites [3]–[6]. However, these models were

developed and validated for thermoset matrix-based composites (*e.g.* carbon/epoxy). Unlike thermoset composites, thermoplastic composites behave quite differently mainly due to the pressure- and time-dependent behaviours of the thermoplastic matrix and its higher level of plasticity.

In this paper, therefore, we propose a systematic approach to determine the RVE of the thermoplastic composites using two methods namely geometrical two-point probability function analysis and Hill-Mandel kinematic homogenization. Next, we implement a set of constitutive models capable of describing the behaviour of thermoplastic composites under various loading conditions with the focus on pressure- and rate-dependent behaviours of thermoplastic matrices. The RVE is then subjected to transverse tension loading and periodical boundary conditions. The model prediction is then validated with the experimental tensile test of $[90]_8$ laminates. The objectives of our analysis are: (i) to establish a high-fidelity micromechanical framework for predicting microscale damage mechanisms and effective mesoscale responses under transverse tension; (ii) to validate the model's predictions with experimental results; and (iii) to use the model as a useful virtual testing tool for material design purposes. In addition, the model should remain as simple as possible, so that it can serve as a pragmatic tool for design optimization.

2. Materials and experimental works

The thermoplastic composite under investigation is provided by SABIC and made of continuous E-glass fibres embedded in an impact copolymer polypropylene (GF/PP). The GF/PP composite comes in the form of unidirectional (UD) prepreg tape with an elementary thickness of 256 ± 1 micrometer. Tensile test specimens of $[90]_8$ laminates were made by stacking the prepreg tapes within a mould and then remelted under a hot press machine with 7.5 bar pressure. The tapes were heated from 23 C (room temperature) to 210 C with a heating rate of 10 C/min, then the temperature was maintained at 210 C for 20 min before being cooled down to room temperature with a cooling rate of 22 C/min. The specimens with a 20 mm width and 110 mm length were then cut from the plate (gauge length was 70 mm). No tabs were used during tensile tests. All tensile tests were performed using an Instron 5944 UTM with a 5 kN load cell. The loading speed was set such that the strain rate in the gage length is 0.001/s. The strains in the in-plane directions were measured using digital image correlation system consist of SensiCam 12-bit CCD camera with TC-12080 bi-telecentric lenses. The acquired images were then processed using VIC-2DTM software.

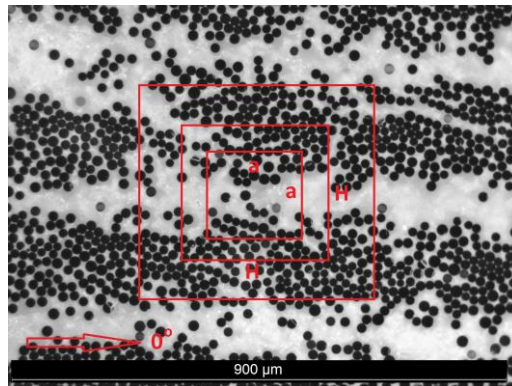


Figure 1. An optical microscopy image of GF/PP composites. a is the windows size and H is the thickness of the elementary ply.

Tensile tests on neat PP were also performed to obtain the tensile properties of neat PP under various strain rates for the proposed micromechanical model. Injection-moulded PP (FPC100) plaques (2 mm

thick) were cut and remelted with the same processing conditions as those used to manufacture the GF/PP laminate, such that both had a similar thermal history. The resulting plates were then shaped using a dog-bone puncher following the ISO 527-2 1BA standard (gauge length and width of 50 mm and 5 mm, respectively). Tensile tests at strain rates of 0.001, 0.01, and 0.1/s were then performed. Readers may refer to Ref. [7] for details on the experimental works on neat PP and GF/PP.

3. Representative volume element: geometrical and mechanical considerations

The spatial distribution of the fibres in composite (*i.e.* the microstructure) largely varies depending on the processing technique and the melt flow index of the matrix. In this study, the investigated tapes are having a unique characteristic of a “layer”-like fibre cluster distribution, whereby fibres disperse and cluster in the form of layers in the middle of the tape, leaving a resin-rich region in the outer part of the ply (see Fig. 1). Obviously, simple unit cell models based on periodical hexagonal [8] or rectangular [9] patterns are not RVE for such a microstructure. Therefore, we propose two approaches to systematically analyse the microstructure from both a geometrical (using two-point probability functions) and a mechanical point of view (by evaluating the eigenvalues of the homogenized elastic tensors). The RVEs are then defined as the minimum observation window which ensures that both the geometrical correlation and the elastic eigenvalues become independent of (1) the size and (2) the location of the observation window on the sample.

3.1. Geometry-guided RVE based on two-point probability function

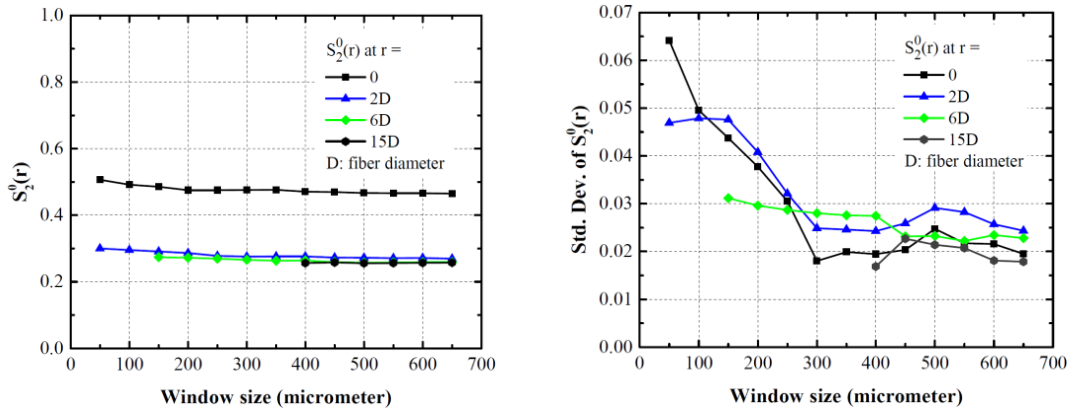


Figure 2. (a) Values of the two-point probability function vs. window sizes and (b) their standard deviations to determine the minimum size of the RVE.

The two-point probability function $S_2(r)$ is defined as the probability of having two endpoints of a line segment of length r lying in the phase of interest (the fiber in this case) when randomly tossed into the sample [10]. For statistically homogeneous media with fibre volume fraction v_f and no long-range order, $S_2(r)$ has the following physical properties:

$$S_2(r = 0) = v_f; \quad S_2(r = \infty) = v_f^2 \quad (1)$$

Using the latter physical interpretation, one can find a distance r_{min} over which the two-point correlation function converges (*i.e.* $S_2(r) - v_f^2 \leq \varepsilon, \forall r \geq r_{min}$, where ε is a small parameter). This so-called “correlation length” r_{min} is the minimum distance between two geometrically uncorrelated points. Then, the size of the RVE of random microstructures should be larger than this geometrical correlation length. Five microscopy images of the fibre distributions were taken from different locations of the cross section of the composite to verify that the RVE was statistically representative.

Due to the layer-like clustering of the fibres, we assumed that the RVE spans over the whole thickness of the elementary ply and therefore, periodicity was assumed in the thickness direction. Next, the search for RVE size will be focused on the 0-degree direction (see Fig. 1) *i.e.* all sampling lines for two-point probability function were tossed along 0-degree orientation only. Fig. 2 shows the ensemble average values of the two-point probability functions and their standard deviations with respect to the window size a . It was found that the minimum size of RVE is $300 \times 255 \mu\text{m}^2$ while the depth of the RVE (*i.e.* the size along fibre direction) is irrelevant because the fibres are assumed to be continuously uniform and the analysis of fibre waviness are not in the scope of this paper.

3.2. Critical size of the RVE based on macroscopic elastic behaviour

Now the RVE will be determined based on stabilization of the eigenvalues of the homogenized elastic tensor. Homogenization is performed using the Hill-Mandel kinematic which assumes the strain is uniform over the RVE boundaries. Once the homogenized elastic tensor is obtained, its six eigenvalues can be plotted with respect to the increasing size of the windows and the RVE can be defined as the size at which all six eigenvalues stabilize.

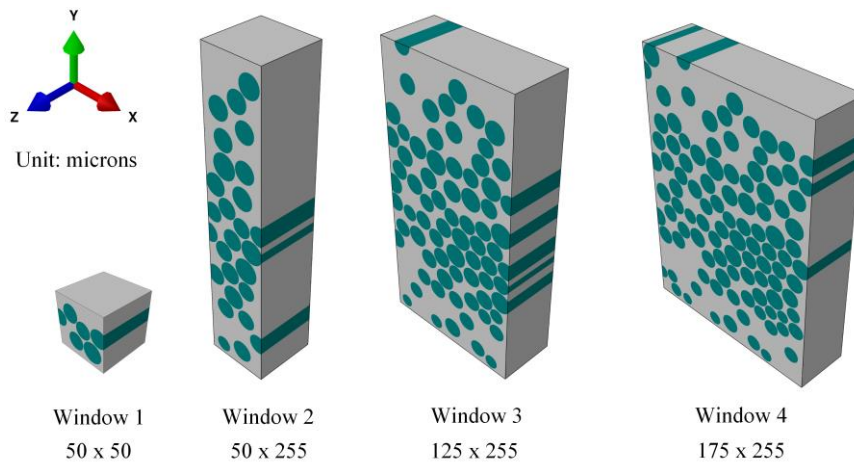


Figure 3. 3D finite element model with various window sizes used to search for the RVE of continuous fibre-reinforced composites

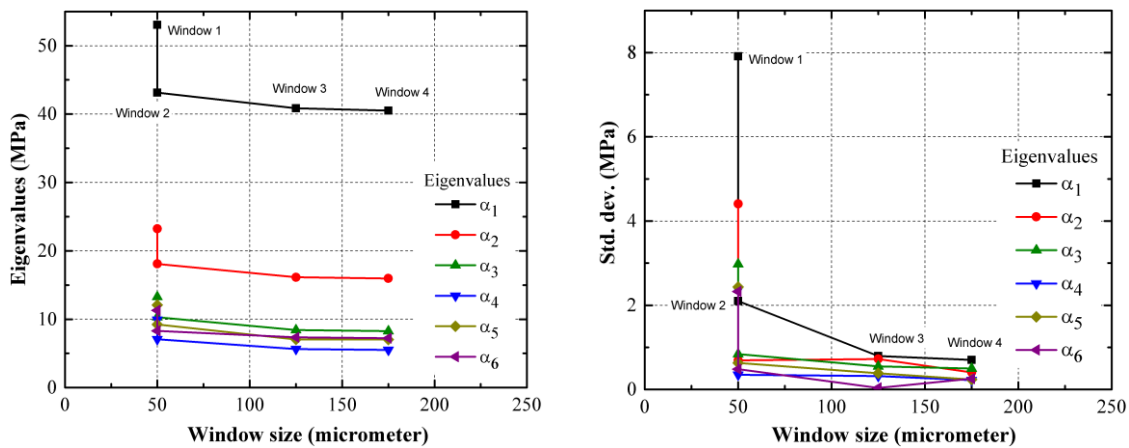


Figure 4. Homogenized stiffness matrix vs. window sizes: (a) eigenvalues and (b) the standard deviations

Excerpt from ISBN 978-3-00-053387-7

We start searching for RVE size from a $50 \times 50 \mu\text{m}^2$ window with increasing thickness up to that of the elementary ply ($50 \times 255 \mu\text{m}^2$). Then the width of window was increased up to $255 \times 255 \mu\text{m}^2$. As discussed earlier, the size of the RVE in the z-direction is irrelevant and for this particular Hill-Mandel kinematic analysis it was arbitrarily chosen to be $50 \mu\text{m}$. The corresponding 3D finite element models, as shown in Fig. 3, were automatically generated using Python script in Abaqus/CAE. Here, both the fibres and matrix are assumed to be linear elastic materials with properties given in Table 1.

Fig. 4 shows the plot of eigenvalues of the homogenized stiffness matrix with respect to the window size. It is clear that the eigenvalues stabilize from a window size of $125 \times 255 \mu\text{m}^2$. Based on these results, the minimum size of the RVE from the mechanical point of view is $125 \times 255 \mu\text{m}^2$. Finally, the critical size of RVE is defined as the size that satisfies both geometrical and mechanical analyses: $300 \times 255 \mu\text{m}^2$ (see Fig. 5a).

4. Finite element model and constitutive equations

4.1. Periodic boundary conditions and model generation

The RVE boundary was imposed with periodical boundary conditions to minimize the edge effect on the homogenization results. A representative of the developed 3D finite element model of the RVE is shown in Fig. 5. The RVE was meshed with 8-node hexahedral elements (C3D8R) with reduced integration points in most areas, and several 6-node prismatic elements (C3D6) to achieve good mesh quality. In addition, the minimum inter-fibre distance was limited to $0.4 \mu\text{m}$ to maintain a good mesh quality. The simulation was carried out using Abaqus Standard V6.12 with automatic time step and additional convergence control settings.

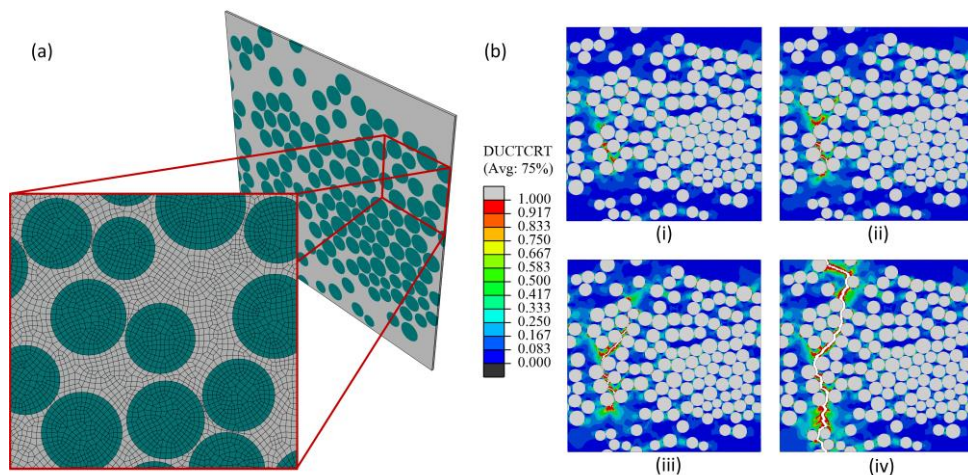


Figure 5. (a) Developed 3D FEM-based RVE model for GF/PP composites and (b) initiation and progression of transverse crack on $[90]_8$ laminates.

4.2. Constitutive models for fibre, matrix and fibre/matrix interface

The RVE is composed of three regions: the glass fibres, the PP matrix and their interfaces. The fibres are modelled as an isotropic linear elastic material while the PP matrix is modelled as an isotropic linear elastic with pressure-dependent plasticity coupled with a ductile damage model. Abaqus [11] built-in hyperbolic Drucker-Prager plasticity model was used due to its capability to consider pressure-dependent plasticity of the matrix [12]. The triaxiality-dependent damage behaviour of PP was taken

into account by setting different damage initiation values for each loading condition. In this study, damage initiation for shear and uniaxial compression was assumed to be three and ten times larger, respectively, than the damage initiation value in the uniaxial tension. The exponential evolution of the damage variable D w.r.t. effective plastic displacement was required for the simulation input.

The interfaces between the fibres and matrix are modelled by the Abaqus 8-node 3D cohesive element (COH3D8) with bilinear traction-separation law [11]. The initial stiffness of the cohesive element is set to be a large number (*i.e.* $K_{nn} = K_{ss} = K_{tt} = 10^7$ GPa/m) to minimize the spurious compliance of undamaged RVE, yet it is small enough to avoid convergence problem due to the ill-posed-ness of the stiffness matrix. Table 1 contains all the required parameters for the proposed micromechanical model.

Table 1. Material parameters for fibre, matrix and fibre/matrix interface

Material property	Glass fibre	PP Matrix	Fibre/matrix interface
Density [kg/m ³]	2580	946	-
Young's modulus [GPa]	72	1.7	10 ⁷ GPa/m ³
Poisson's ratio	0.22	0.4	-
Pressure dependent angle [°]	-	31.5	-
Plastic hardening data	-	See Ref. [7]	-
Critical equivalent plastic strain $\varepsilon_{eq,cr}^p$	-	0.164 (uniaxial tension)	-
Maximum plastic displacement after damage initiation [micrometer]	-	0.1315	-
Maximum strength [MPa]	-	-	20 (isotropic)
Critical energy release rate G_c [J/m ²]	-	-	10

5. Results and discussions

5.1. Experimental validations

Homogenized mesoscale stress-strain response obtained from the proposed micromechanical model will be validated against the experimental results in this subsection. Tensile test on [90]₈ laminates at strain rate 0.001/s have been conducted [7] and the corresponding prediction of the micromechanical RVE will be discussed. Fig. 6a shows the model prediction of [90]₈ laminates under transverse tension at strain rate 0.001/s. The model prediction is in very excellent agreement with the experimental results. The proposed model is capable of predicting both linear elastic and nonlinear plastic responses of the RVE accurately. The average of predicted Young's modulus of 4.41 ± 0.10 GPa for the transverse direction was in good agreement with the experimental results (*i.e.* 4.43 ± 0.19 GPa [7]).

Fig. 5b shows the contour plot of variable ω in the matrix of a deformed RVE of [90]₈ laminates at several macroscopic strain levels. The contour ω gives information on the level of plasticity in the matrix and how close it is to the damage initiation criteria. Red in the plot means that these elements are close to or already damaged. Note how the damage initiates and localizes at regions where fibres are packed closely together (see Fig. 5b). The presence of closely located fibres generates high stress concentration in the matrix in between. Therefore, inter-fibre distance is a very important factor in determining the failure behaviour of UD laminate under transverse tension. Thus, a manufacturing strategy to generate good spreading of fibres is inevitably required to improve the performance of the thermoplastic composite.

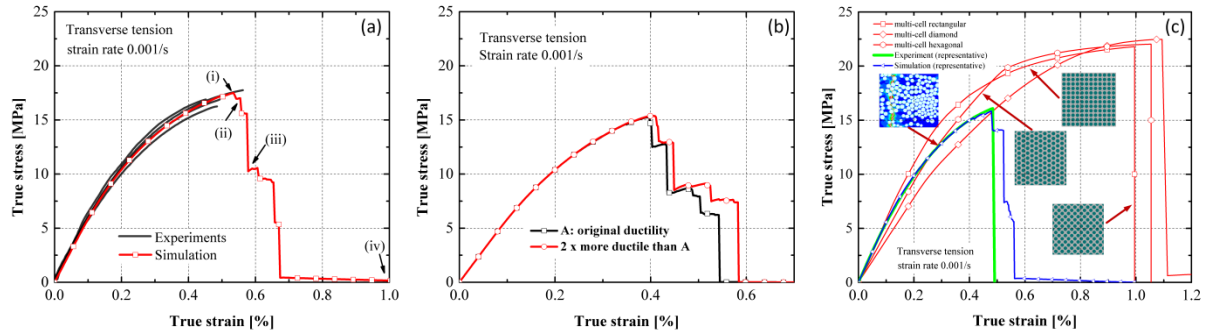


Figure 6. (a) Model prediction vs. experimental results, (b) effect of matrix ductility and (c) effect of fibre spatial distributions (inter-fibre distance)

5.2. Understanding the effect of matrix properties

The role of matrix ductility was explored by increasing the damage initiation criteria, ε_p^{cr} , two times higher than its original value (i.e. $\varepsilon_{p,new}^{cr} = 2 \times 0.0164$). While the interface properties were set to $t_{max} = 20$ MPa and $G_c = 3.7$ J/m² and all other parameters were kept the same as in Table 1. Fig. 6b shows the homogenized stress-strain curve for the two matrices with different ductility. In majority, the stress-strain curves prior to maximum loading are superimposed. This is due to the nature of the damage developed on UD laminates under transverse tension which is local and propagating rapidly over a narrow band. Hence, the effect of matrix ductility is negligible in terms of homogenized stress-strain curve. Therefore, making a more ductile matrix is not the best strategy for improving the ductility of UD laminates under transverse tension.

5.3. Understanding the effect of microstructures

The effect of microstructures *i.e.* fibre spatial distribution was investigated. The responses of composites obtained using statistical RVE were compared with results of using the simple periodical networks (hexagonal, diamond and rectangle). In simple periodical networks, the fibre diameter was kept uniform equal to the average diameter of fibres in statistical RVE (16.4 μ m) and the size of each simple periodical unit cell is set such that the volume fraction is 46.5%, *i.e.* the volume fraction of the statistical RVE. Comparison between the statistical RVE and the simple periodic unit cell model will give clues about the importance of the inter-fibre distance and the resulting stress-concentration on the damage behaviour of composite materials. Fig. 6c shows the effect of inter-fibre distance on the global response of the UD laminate under transverse tension. Generally, for a simple unit cell model, the maximum stress attainable is higher than the prediction with statistical RVEs. In addition, the failure strain predicted by a simple unit cell model shows a much delayed failure point. This is due to the fact that in the case of a simple periodical network, the distribution is homogeneous and the stress concentration effect is minimized. This clearly demonstrated the need to improve the technology to control the dispersion of fibres because it significantly affects the damage initiation of the composites.

6. Conclusions

We performed micromechanical damage modelling of glass fibre-reinforced thermoplastic composite under transverse tension to study the microscopic failure mechanisms and their effect on the mesoscale response. We start by systematically determining the RVE for such microstructures and then a set of constitutive models capable of describing the behaviour of GF/PP under various loading conditions was implemented. The responses of the RVE were then validated against the experimental result of

[90]₈ laminates under transverse tension. The model predictions were in an excellent agreement with experimental results. Parametric studies were then performed to explain the most dominant factors in the damage behaviour of thermoplastic composites. Several conclusions can be made in general and might be helpful for material design point of view:

- ✓ Matrix ductility does not significantly improve the performance of the [90]₈ laminates under transverse tension.
- ✓ Inter-fibre distance plays a significant role in determining the damage initiation and progression.

Acknowledgements

We acknowledge SABIC for providing research funds and raw materials. We also acknowledge support from Baseline Research Fund from King Abdullah University of Science and Technology.

References

- [1] J. Osborne, “Automotive Composites – in Touch with Lighter and More Flexible Solutions,” *Met. Finish.*, vol. 111, no. 2, pp. 26–30, 2013.
- [2] G. Lubineau, “A pyramidal modeling scheme for laminates-identification of transverse cracking,” *Int. J. Damage Mech.*, vol. 19, no. 4, pp. 499–518, 2010.
- [3] L. Yang, Y. Yan, Y. Liu, and Z. Ran, “Microscopic failure mechanisms of fiber-reinforced polymer composites under transverse tension and compression,” *Compos. Sci. Technol.*, vol. 72, no. 15, pp. 1818–1825, Oct. 2012.
- [4] A. R. Melro, P. P. Camanho, F. M. Andrade Pires, and S. T. Pinho, “Micromechanical analysis of polymer composites reinforced by unidirectional fibres: Part I – Constitutive modelling,” *Int. J. Solids Struct.*, vol. 50, no. 11–12, pp. 1897–1905, Jun. 2013.
- [5] G. Soni, R. Singh, M. Mitra, and B. G. Falzon, “Modelling matrix damage and fibre–matrix interfacial decohesion in composite laminates via a multi-fibre multi-layer representative volume element (M2RVE),” *Int. J. Solids Struct.*, vol. 51, no. 2, pp. 449–461, Jan. 2014.
- [6] J. Zhang, L. Zhou, Y. Chen, L. Zhao, and B. Fei, “A micromechanics-based degradation model for composite progressive damage analysis,” *J. Compos. Mater.*, Sep. 2015.
- [7] A. Yudhanto, G. Lubineau, H. Wafai, M. Mülle, D. A. Pulungan, R. Yaldiz, and N. Verghese, “Monotonic and cyclic responses of impact polypropylene and continuous glass fiber-reinforced impact polypropylene composites at different strain rates,” *Polym. Test.*, Mar. 2016.
- [8] S. Y. Hsu, T. J. Vogler, and S. Kyriakides, “Inelastic behavior of an AS4/PEEK composite under combined transverse compression and shear. Part II: modeling,” *Int. J. Plast.*, vol. 15, no. 8, pp. 807–836, Jan. 1999.
- [9] Y. Zhang, Z. Xia, and F. Ellyin, “Nonlinear viscoelastic micromechanical analysis of fibre-reinforced polymer laminates with damage evolution,” *Int. J. Solids Struct.*, vol. 42, no. 2, pp. 591–604, Jan. 2005.
- [10] S. Torquato, *Random heterogeneous materials: microstructure and macroscopic properties*, vol. 16. Springer Science & Business Media, 2002.
- [11] Dassault Systemes Simulia Corp., *Abaqus 6.12 Documentation*. 2012.
- [12] M. Jerabek, D. Tscharnuter, Z. Major, K. Ravi-Chandar, and R. W. Lang, “Multiaxial yield behaviour of polypropylene,” *EPJ Web Conf.*, vol. 6, p. 03005, Jun. 2010.